Ternary Phase Equilibrium Diagrams for *o*- and *p*-Chlorobenzoic Acids and Their Complex with Piperazine in Methanol

Asghar Lashanizadegan,‡ Narayan S. Tavare, Mehrdad Manteghian,§ and David M. T. Newsham*,†

Department of Chemical Engineering, University of Bradford, West Yorkshire, BD7 1DP, U.K.

During the study of the separation of *o*- and *p*-chlorobenzoic acids by a two-phase process of dissociation extractive crystallization using methanol and piperazine as a solvent and reagent, respectively, the ternary phase equilibrium diagrams for the *o*-chlorobenzoic acid + methanol + *p*-chlorobenzoic acid system were constructed at 10, 20, and 30 °C. Equilibrium chlorobenzoic acid + piperazine complex concentrations in the solution phase from three series of batch equilibrium precipitation experiments performed at different temperatures were represented on the ternary diagrams. The results indicated the potential efficacy of the separation technique for this system.

Introduction

In the manufacture of chemical and pharmaceutical products, the wide variety of isomeric or closely related mixtures of organic compounds that are encountered often require their separation into nearly pure components. The present research was motivated by the problem of the separation of *o*- and *p*-chlorobenzoic acids from their mixtures using the addition of a third component that augments the ease of separation. Chlorobenzoic acids, used as intermediate chemicals, can be synthesized by the oxidation of a mixture of chlorotoluenes. The end product will generally contain an isomeric mixture of mainly *o*- and *p*-chlorobenzoic acids and cannot be separated by conventional separation techniques. The melting points of *o*- and *p*-chlorobenzoic acids are 142 °C and 243 °C, respectively. These two components form a simple eutectic system. The separation of *o*- and *p*-chlorobenzoic acid mixtures has been studied extensively in the literature [Laddha and Sharma,[1] by the dissociation leaching (or extraction) method; Gaikar and Sharma[2] by controlled leaching with hydrotrope solutions; Phatak and Gaikar[3] and Tavare and co-workers (Colônia et al.,[4−6] Dixit et al.[7,8]) through hydrotropy; Lashanizadegan and Tavare[9] and Lashanizadegan et al.[10] by the process of dissociation extractive crystallization]. Recently, Lashanizadegan et al.[10] developed a predictive model based on a modified UNIFAC group contribution method. This model can be used to evaluate the concentrations of all species as well as the effectiveness of the process, thus providing the theoretical basis for a better understanding of the solution phase behavior. For the separation of *o*- and *p*-chlorobenzoic acid mixtures, methanol and piperazine were chosen as solvent and reagent, respectively. Selection of methanol was based on a rational thermodynamic approach in screening the solvents by utilizing a modified UNIFAC group contribution method. When solid piperazine, in a stoichiometrically deficient

amount, is added to the solution of chlorobenzoic acids in methanol, it reacts preferentially after solubilization with *o*-chlorobenzoic acid and forms an *o*-chlorobenzoic acid + piperazine complex compound due to the stronger acidic character of *o*-chlorobenzoic acid. The reaction product is sparingly soluble in the solution phase and precipitates out from the reaction mixture. As the complex compound precipitates out from the reaction mixture, the reaction continues to form more of the complex compound in order to establish chemical equilibrium. This paper is concerned with the determination of relevant solubility data and construction of ternary solid−liquid-phase equilibrium diagrams for the *o*-chlorobenzoic acid + methanol + *p*-chlorobenzoic acid system at various temperatures, and the effectiveness of the separation of chlorobenzoic acid mixtures in methanol at various concentrations and temperatures. For the dissociation extractive crystallization process, a ternary solid−liquid-phase equilibrium diagram can be used to represent the temperature and concentration regions of interest for a desired separation.

Experimental Section

The construction of the ternary solid−liquid-phase equilibrium diagram for the *o*-chlorobenzoic acid + methanol + *p*-chlorobenzoic acid system at any temperature requires the determination of (a) the solubilities of pure *o*- and *p*-chlorobenzoic acids in methanol, (b) the solubility curve of *o*-chlorobenzoic acid in methanol in the presence of *p*-chlorobenzoic acid (i.e., the *o*-chlorobenzoic acid saturation curve with undersaturated *p*-chlorobenzoic acid), (c) the solubility of *p*-chlorobenzoic acid in methanol in the presence of *o*-chlorobenzoic acid (i.e., the *p*-chlorobenzoic acid saturation curve with undersaturated *o*-chlorobenzoic acid), and (d) the eutonic (or two-component saturation) point, that is, the point at which methanol is saturated with respect to both *o*- and *p*-chlorobenzoic acids. Crystalline *o*- and *p*-chlorobenzoic acids were Fluka AR grade (>98% purity), piperazine (>99% purity) was AR grade from Aldrich, and AR grade methanol was used for the experiments while HPLC grade methanol was used for preparing the mobile phase in HPLC analyses. To obtain the chlorobenzoic acid + piperazine complex compound, a known amount of *o*- or *p*-chlorobenzoic acid was added to methanol

† Department of Chemical Engineering, UMIST, Manchester M60 1QD, U.K.
‡ Department of Chemistry, Shiraz University, Shiraz 71454, Iran.
§ Department of Chemical Engineering, Tarbiat Modarres University, Tehran 4838, Iran.
* Corresponding author. E-mail: d.newshamumist.ac.uk. Fax:0161-200 4399.

below the saturation concentration at ambient temperature and a stoichiometric amount of piperazine was added to the solution while stirring. The reaction between the acid and piperazine yielded a slurry. After equilibration (i.e., 2 h of stirring) the slurry was filtered through filter paper (Whatman #1) using a Büchner filter and the resulting solid chlorobenzoic acid + piperazine complex compound was dried in an oven at 70 °C.

Solubility Data. The solubilities of solid *o*- and *p*-chlorobenzoic acids in methanol were determined by the mass disappearance method (Geetha et al.[11]). To determine the solubility, the mass of dissolved material in the solution during the equilibration step was evaluated as the difference between the masses of the initial charge and the final residue. In the equilibration step, a known and excess amount of solid *p*-chlorobenzoic acid (~5−10 g) was charged into 100 g of solvent contained in a jacketed vessel of 250 mL capacity. The resulting suspension was sealed and magnetically stirred for equilibration for at least 6 h. The temperature was maintained constant by circulating water from a water bath around the jacketed vessel. The bath temperature was controlled with an accuracy of ±0.1 °C. Because of the temperature drop in the circulation loop, the actual solution temperature was checked by a thermometer having an accuracy of ±0.1 °C. After equilibration (i.e., ~6 h stirring), the slurry was filtered through filter paper (Whatman #1) at constant temperature and the residue dried overnight in an oven at 70 °C and weighed. The solubility was determined from the difference in mass between the initial charge and the final residue. Solubilities of *o*-chlorobenzoic acid in methanol are relatively high, and in this case, the solubility determination was carried out on a small scale. An excess amount of *o*-chlorobenzoic acid (~6−10 g) was charged into ~8 g of the solvent contained in a small vial (typically 20 mL). The vial was sealed and fixed in the jacketed vessel, whose temperature was maintained constant by the water bath (see Figure 1). The resulting suspension was magnetically stirred for at least 6 h to achieve equilibration and then was allowed to stand for 1 h at that temperature so that any finely dispersed particles could settle. The clear saturated solution over the solid phase was removed with a syringe and weighed. The residue that contained the saturated solution and solid *o*-chlorobenzoic acid was weighed and dried overnight in an oven at 70 °C and then weighed again. Knowing the mass of the residue before and after drying (R_1 and R_2, respectively) as well as the initial masses of *o*-chlorobenzoic acid and the solvent ($m_{o\text{-CBA}}$ and m_{solvent}, respectively), the solubility of *o*-chlorobenzoic acid in methanol was determined.

$$\text{solubility (mass \%)} = \frac{m_{o\text{-CBA}} - R_2}{m_{\text{solvent}} - R_i + m_{o\text{-CBA}}} \times 100 \quad (1)$$

Using these procedures, solubilities of pure *o*- and *p*-chlorobenzoic acids were determined at 10, 20, and 30 °C. For the construction of the solid−liquid equilibrium ternary diagram for the *o*-chlorobenzoic acid + methanol + *p*-chlorobenzoic acid system, almost all experiments were performed on the small scale to determine all the necessary saturation conditions. For the eutonic point, known excess amounts of *o*-chlorobenzoic acid (~ 6−100 g) and *p*-chlorobenzoic acid (~0.8−1.2 g) were equilibrated with a known amount of methanol for a minimum of 6 h. The slurry was then maintained at constant temperature without stirring for 1 h in order to allow finely dispersed solid particles to settle. A known amount of clear saturated
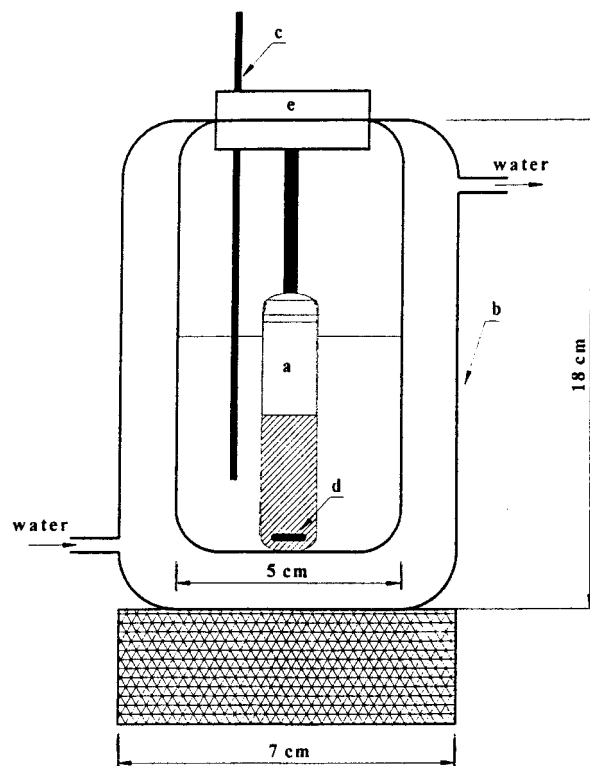

Figure 1. Solubility determination on a small scale: a, vial (~20 mL); b, jacketed vessel; c, thermometer; d, magnetic stirrer; e, rubber bung.

liquid was withdrawn with a syringe, weighed, and diluted for HPLC analysis in order to determine the concentration of the acids at the eutonic point. To determine the data points on the *o*- or *p*- saturation curves, known amounts of *o*- or *p*-chlorobenzoic acid in methanol were prepared. The solubilities of *o*- or *p*-chlorobenzoic acid in solutions having known *p*- or *o*-chlorobenzoic acid concentrations (below the saturation point) were also determined by the mass disappearance method. In some experiments, HPLC analysis was used to check the solution concentrations. Both *o*- and *p*-chlorobenzoic acids in the mixtures were quantitatively analyzed by HPLC on a Gilson chromatograph. For the analysis, the column used was 25 cm long and 4.6 mm diameter packed with Chromosphere C_{18} (ODS2 5 μm). The mobile phase used for the analysis was a mixture of 65 vol % methanol and 35 vol % distilled water containing 5 vol % phosphoric acid with a flow rate of 1−2 mL/min. The mobile phase was filtered twice through filter paper (Whatman, pore size 0.2 μm) and then degassed in an ultrasonic bath where the dissolved gases in the solution were removed. High pressure (~140 MPa) was generated by a positive displacement pump in order to force the mobile phase (the eluent) through the column. The detector that was placed at the end of the column responded to solute concentrations by absorption of ultraviolet light at a wavelength of 260 nm. Therefore, continuous detection and quantitative determination of concentrations were readily accomplished as the eluent passed through the detector. Chromatograms and integrated data were recorded with a Gilson integrator, which provided measurements of relative peak areas. Before injecting the samples into the chromatograph, they were diluted with HPLC grade methanol to a suitable concentration and then filtered through a syringe membrane filter (13 mm diameter, Whatman, pore size 0.1 μm) with a cellulose nitrate medium. The required concentration of the acids in the samples for direct injection to the chromatograph was in

Table 1. Solubility Data for the *o*-Chlorobenzoic Acid (1) + Methanol (2) + *p*-Chlorobenzoic Acid (3) System

$t = 10\ °C$		$t = 20\ °C$		$t = 30\ °C$	
measured saturation concentrations in the solution phase, mass %					
x_1	x_3	x_1	x_3	x_1	x_3
Eutonic Point		Eutonic Point		Eutonic Point	
31.15	4.04	37.71	5.36	43.83	7.14
p-Chlorobenzoic Acid Saturation Curve					
0.00	2.66	0.00	3.30	0.00	3.52
5.88	2.75	4.20	3.41	5.88	3.79
11.11	2.89	7.52	3.27	11.11	4.31
15.79	2.94	10.62	3.58	15.79	4.33
20.00	3.14	24.00	4.43	31.25	4.40
27.27	3.79	20.00	4.91	27.27	5.33
		24.53	5.51	33.33	6.33
		28.57	6.18		
		31.62	4.89		
		34.43	5.30		
o-Chlorobenzoic Acid Saturation Curve					
31.33	0.00	37.65	0.00	43.15	0.00
30.92	1.27	37.32	0.09	42.94	1.23
31.10	2.44	37.38	1.66	42.79	2.44
		37.69	3.27	43.79	3.04
		37.61	4.99		
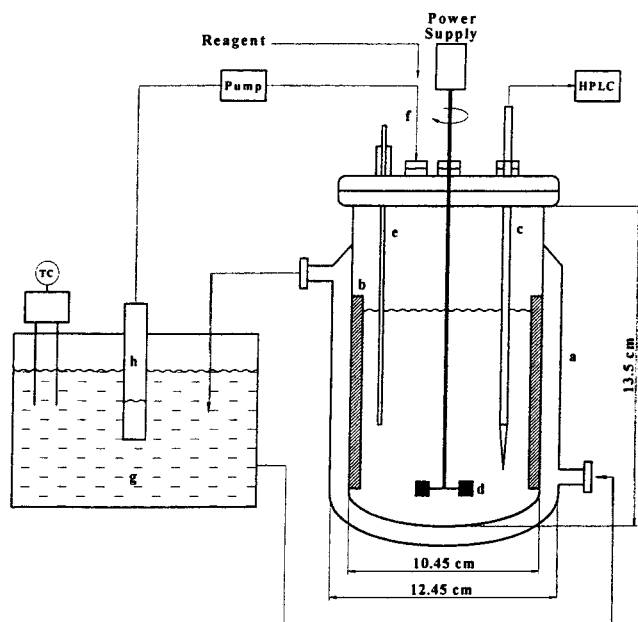
Figure 2. Schematic diagram of the apparatus used for the separation experiments: a, jacketed vessel; b, baffles; c, liquid sampling to analyzer; d, six bladed turbine impeller; e, thermometer; f, reagent addition port; g, water bath; h, liquid reagent.

the range (0.2−1.8) mg of solute/g of solvent, and the injection volume was 100 μL.

All the experimental results are included in Table 1. The estimated accuracy of the solubility values, based on error analysis and repeated observations, was within ±2%. In a few experiments, a closure on component mass balance was checked and found satisfactory within the range of experimental errors. Solubilities of both these pure components and their mixture at eutonic points increased with temperature. The solubility of the *o*-isomer is much higher than that of the *p*-isomer. The ratio of the solubilities (*o*-/*p*-) increases slightly from 16.7 at 10 °C to 20.8 at 30 °C. Probably methanol can better accommodate an *o*-component in the solution phase rather than its symmetrically structured *p*-component. Solubilities of both these components increased in the presence of the other. For *p*- and

Table 2. Batch Separation Experiments for the *o*-Chlorobenzoic Acid (1) + Methanol (2) + *p*-Chlorobenzoic Acid (3) System: Component Compositions (x_i, Piperazine-Free Mass %)

initial composition		final composition	
x_1	x_3	x_1	x_3
$t = 20\ °C$			
0.88	0.88	0.66	0.95
1.25	0.88	0.51	0.89
1.86	0.88	0.52	0.93
2.47	0.88	0.42	0.82
3.66	0.88	0.48	0.84
1.86	1.25	0.49	1.24
2.47	1.25	0.51	1.30
3.66	1.25	0.48	1.18
0.88	1.59	0.47	1.41
1.25	1.59	0.53	1.72
1.86	1.59	0.52	1.67
2.47	1.59	0.49	1.46
3.66	1.59	0.52	1.69
1.86	2.47	0.54	2.57
2.47	2.47	0.49	2.23
3.66	2.47	0.55	2.48
0.88	3.07	0.59	2.87
1.86	3.07	0.53	3.06
2.47	3.07	0.52	3.02
3.66	3.07	0.57	3.03
3.66	3.07	0.55	3.14
5.95	3.07	0.40	2.53
$t = 10\ °C$			
1.25	1.25	0.52	1.12
2.47	1.25	0.53	1.23
3.66	1.25	0.40	1.37
1.25	2.47	0.41	2.46
2.47	2.47	0.35	2.38
3.66	2.47	0.37	2.40
4.82	2.47	0.49	2.41
$t = 3\ °C$			
2.47	0.88	0.20	0.75
3.66	0.91	0.28	0.87
1.37	1.25	0.30	1.36
2.47	1.25	0.32	1.22
3.66	1.25	0.28	1.24
1.25	2.47	0.30	2.40
2.47	2.47	0.31	2.28
3.66	2.47	0.33	2.46

o-chlorobenzoic acid saturation curves, concentrations of the other component (i.e., *o*- and *p*-chlorobenzoic acid, respectively) were increased between the pure component and the eutonic point by a predecided interval in order to obtain an adequate number of data points on the curves. As *o*-chlorobenzoic acid is much more soluble than *p*-chlorobenzoic acid, between 6 and 10 data points were chosen for *p*-chlorobenzoic acid and between 3 and 5 for *o*-chlorobenzoic acid.

Separation Experiments. Separations of *o*- and *p*-chlorobenzoic acids from their mixtures were made by the two-phase dissociation extractive crystallization process. A series of separation experiments were performed in a 1 L jacketed vessel fitted with four full baffles and sealed with a flat glass lid having four entry nozzles to house the impeller, the thermometer, the reagent inlet, and the sampling port. The schematic diagram of the experimental setup is shown in Figure 2. A 34 mm diameter stainless steel six bladed turbine impeller was mounted at the central axis with a clearance of about 1 cm from the bottom. The temperature within the reactor was maintained at a constant value by circulating water from the temperature-controlled water bath through the jacket.

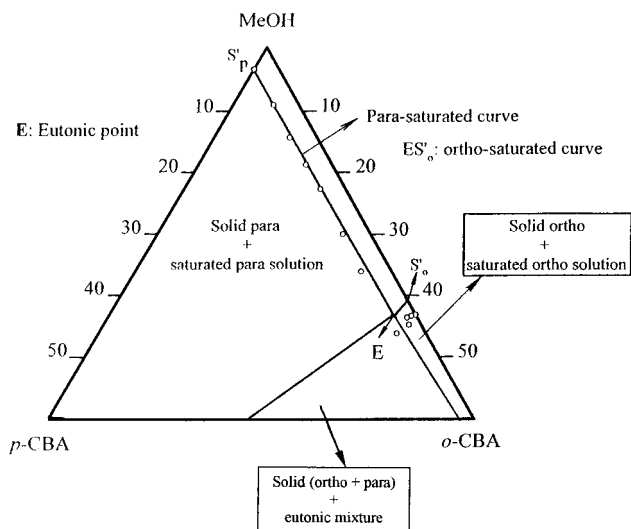In a typical run, a clear solution having known concentrations of *o*- and *p*-chlorobenzoic acids in methanol (~500

Figure 3. Ternary phase equilibrium diagram for the *o*-chlorobenzoic acid (*o*-CBA) + methanol + *p*-chlorobenzoic acid (*p*-CBA) system at 30 °C. All concentrations are in mass %: ○, experimental data; —, predicted phase boundaries.

Figure 4. Ternary phase equilibrium diagram for the *o*-chlorobenzoic acid (*o*-CBA) + methanol + *p*-chlorobenzoic acid (*p*-CBA) system at 20 °C. All concentrations are in mass %: ○, experimental data; —, predicted phase boundaries.

Figure 5. Ternary phase equilibrium diagram for the *o*-chlorobenzoic acid (*o*-CBA) + methanol + *p*-chlorobenzoic acid (*p*-CBA) system at 10 °C. All concentrations are in mass %: ○, experimental data; —, predicted phase boundaries.

g) was stirred continuously in the reactor at the desired working temperature and a stoichiometrically deficient amount of piperazine was added to the solution. After 3 h, the agitation was stopped and the solution was allowed to stand for 1 h at constant temperature so that any finely dispersed solid particles could settle. A known amount of clear liquid solution was removed with a syringe, weighed, and diluted for HPLC analysis in order to determine the concentrations of *o*- and *p*-chlorobenzoic acids. The remaining solid–liquid mixture was filtered and the residue dried and weighed in order to check the accuracy of the analytical results by a mass balance. On average, the agreement was within 4.7%. However, inspection of Figures 6 and 7 and Table 2 shows that errors of up to 0.15 mass % of *o*-chlorobenzoic acid and *p*-chlorobenzoic acid do occur. Altogether, 42 separation experiments were performed at various concentrations of *o*- and *p*-chlorobenzoic acids at 10, 20, and 30 °C, and the results are given in Table 2. These experiments were performed by changing the initial compositions of *o*- and *p*-chlorobenzoic acids systematically over the ranges 0.78–5.89 mass % for *o*-chlorobenzoic acid and 0.78–3.04 mass % for *p*-chlorobenzoic acid.

Results and Discussion

Ternary Phase Equilibrium Diagrams. To explore the temperature and concentration regions of interest for a desired separation, it is convenient to illustrate the dissociation extractive crystallization process on a ternary solid–liquid phase diagram. This provides a visual description of the phase behavior and is very helpful in understanding the phase equilibria. The phase diagram also provides information regarding the thermodynamic equilibrium restrictions imposed on the separation.

Using the results in Table 1, three ternary solid–liquid-phase equilibrium diagrams at (10, 20, and 30) °C were constructed and their enlarged methanol apex regions are shown in Figures 3–5, respectively. Also included in these figures are the predicted curves from the proposed thermodynamic model based on a modified UNIFAC group contribution method (Lashanizadegan et al.[11]). In this model, the precipitation and chemical equilibria are evaluated with activity coefficients evaluated from the UNIFAC model. The latter was modified in the sense that *o*-chlorobenzoic acid and *p*-chlorobenzoic acid were assigned
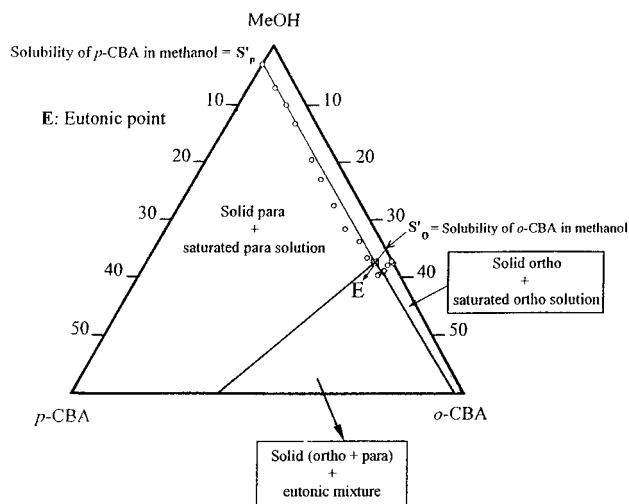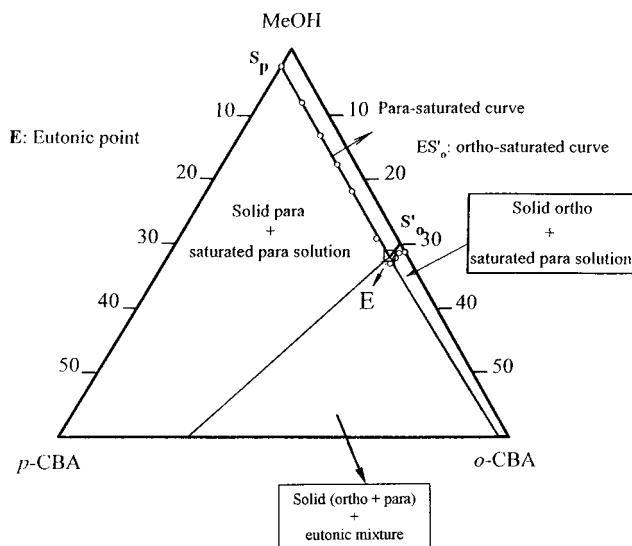
as separate subgroups with relevant parameters obtained from their solubilities in various solvents. In these figures, points S′$_0$ and S′$_p$ represent the solubilities of *o*- and *p*-chlorobenzoic acids in pure methanol. Point E is the eutonic or invariant point at which the solution phase is saturated with both *o*- and *p*-chlorobenzoic acids. ES′$_0$ and ES′$_p$ are the *o*- and *p*-chlorobenzoic acid saturation curves, respectively. The average relative errors between the experimental and predicted values of the *o*- and *p*-chlorobenzoic acid solubility curves were 1.2 and 4.0%, respectively. The ternary diagram is divided into four regions. There are two primary crystallization regions of *p*- and *o*-chlorobenzoic acids (*p*-CBA–ES′$_p$ and *o*-CBA–ES′$_0$). The third region (*o*-CBA–*p*-CBA-E) contains a solution of eutonic composition and solid *o*- and *p*-chlorobenzoic acids, and the fourth region (S′$_p$ES′$_0$–MeOH) corresponds to undersaturated solutions of *o*- and *p*-chlorobenzoic acids.

Representation of Chlorobenzoic Acid + Piperazine Complex Equilibrium Curves. The equilibrium experiments can be represented on a ternary diagram by plotting the initial feed and the final compositions in the liquid
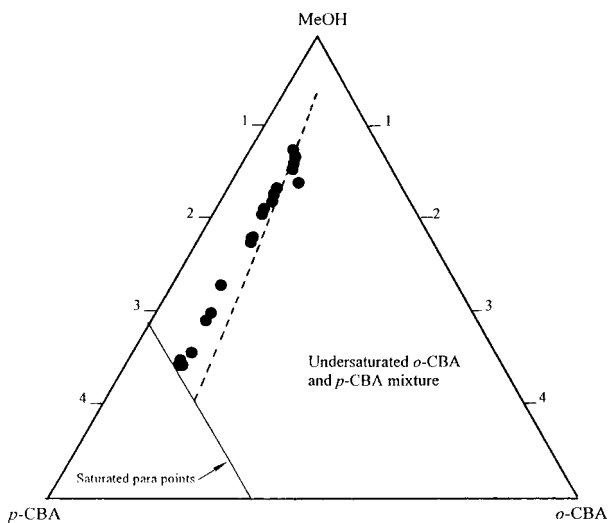
Figure 6. Equilibrium concentrations of chlorobenzoic acid + piperazine complexes at 20 °C. All concentrations are expressed in piperazine-free mass %: ●, experimental equilibrium concentration; - - -, predicted equilibrium curve.
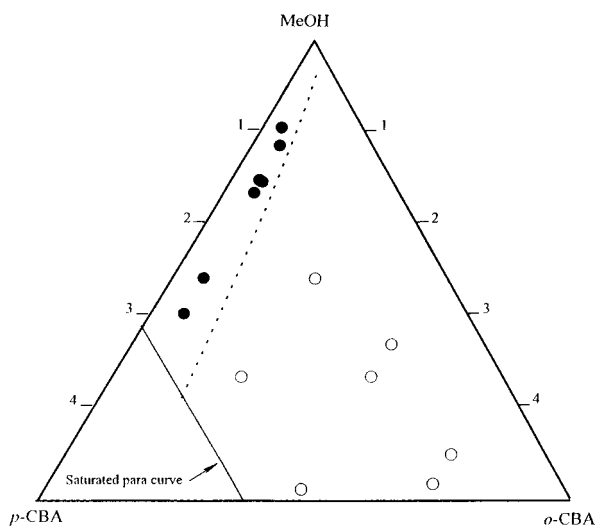

Figure 7. Equilibrium concentrations of chlorobenzoic acid + piperazine complexes at 3 °C. All concentrations are expressed in piperazine-free mass %: ●, experimental equilibrium concentration; ○, initial concentration; - - -, predicted equilibrium curve.

phase after equilibration. The final product concentrations in the solution phase from two sets of equilibrium precipitation experiments given in Table 2 are shown in Figures 6 and 7 for two operating temperatures (20 °C and 3 °C, respectively). Also included in these figures is the locus of the theoretically predicted equilibrium data points for both the *o*- and *p*-chlorobenzoic acid complexes. The average relative error between the final experimentally observed and theoretically predicted saturation composition is about 14%. Also denoted in Figure 7 are the initial feed compositions. When a stoichiometrically deficient amount of piperazine is added to a mixture of *o*- and *p*-chlorobenzoic acids in methanol, the system contains four components. In all these experiments a stoichiometrically deficient amount of piperazine with respect to *o*-chlorobenzoic acid is added to the initial *o*- and *p*-chlorobenzoic acid solution in methanol. Not only is *o*-chlorobenzoic acid a stronger acid than *p*-chlorobenzoic acid but also its reaction complex with piperazine is less soluble than that of *p*-chlorobenzoic acid. Owing to the sparingly soluble complex compounds, almost all the piperazine associated with complexes precipitates

and therefore the total concentration of piperazine remaining in the free or unprotonated form and associated with the complexes in the solution phase is very small. The concentration of free or unprotonated piperazine in the solution can be assumed to be negligible. To represent the process on a ternary diagram, it is necessary to express the concentrations of the complex on a piperazine-free basis. Thus, the acids in the final product are in the form of free acids and complex compound and the apparent acid concentration is the sum of free acid and acids combined with the complex compound. Such a representation is useful and allows the estimation of the effectiveness of the process without recourse to computational work. It is interesting to note that, for a fixed initial *o*-chlorobenzoic acid concentration, the operating line joining the feed and product composition would be a straight line parallel to the *p*-chlorobenzoic acid saturation line, while, for a fixed initial *p*-chlorobenzoic acid concentration, the final composition is independent of the feed point. Using this process, high recoveries and purities of *o*-chlorobenzoic acid can be obtained over a wide range of concentrations. For example, the separation of a mixture containing the two acids (having initial concentrations of 3.66 mass % *o*-chlorobenzoic acid and 2.47 mass % *p*-chlorobenzoic acid) yielded a final mother liquor containing 0.33 mass % *o*-chlorobenzoic acid and 2.46 mass % *p*-chlorobenzoic acid.

Conclusions

Solubility data for the pure components and component saturation curves for mixtures and the two-component saturation point were determined for solutions of *o*- and *p*-chlorobenzoic acids in methanol. The ternary solid–liquid-phase equilibrium diagrams for the *o*-chlorobenzoic acid + methanol + *p*-chlorobenzoic acid system were constructed at three temperatures. The separation of *o*- and *p*-chlorobenzoic acids by a two-phase process of dissociation extractive crystallization using methanol and piperazine as a solvent and reagent, respectively, was investigated. Chlorobenzoic acid + piperazine complex concentrations in the solution phase achieved at equilibrium in three series of batch precipitation experiments performed at different temperatures were represented on the ternary diagrams. For this system, the separation technique appears to be potentially useful.

Acknowledgment

Literature Cited

(1) Laddha, S. S.; Sharma, M. M. Separation of close boiling organic acids and bases by dissociation extraction: chlorophenols, *n*-alkylphenols, chlorobenzoic acids. *J. Appl. Chem. Technol. Biotechnol.* **1978**, *28*, 69–78.

(2) Gaikar, V. G.; Sharma, M. M. Separations through reactions and other novel strategies. *Sep. Purif. Methods* **1989**, *18*, 111–176.

(3) Phatak, P. V.; Gaikar V. G. Solubility of *o*- and *p*-chlorobenzoic acids in hydrotrope solutions. *J. Chem. Eng. Data* **1993**, *38*, 217–220.

(4) Colônia, E. J.; Dixit, A. B.; Tavare, N. S. Separation of *o*- and *p*-chlorobenzoic acids: hydrotropy and precipitation. *J. Cryst. Growth* **1996**, *166*, 976–980.

(5) Colônia, E. J.; Dixit, A. B.; Tavare, N. S. Separation of chlorobenzoic acids through hydrotropy. *Ind. Eng. Chem. Res.* **1998**, *37*, 1956–1969.

(6) Colônia, E. J.; Dixit, A. B.; Tavare, N. S. Phase relations of *o*- and *p*-chlorobenzoic acids in hydrotrope solutions. *J. Chem. Eng. Data* **1998**, *43*, 220–225.

(7) Dixit, A. B.; Colônia, E. J.; Tavare, N. S. Selective precipitation of *p*-chlorobenzoic acid. In Biscans, B., Garside, J., Eds.; *Proc. 13th Symp. on Industrial Crystallization*, Toulouse, 1996; Association pour la Promotion die Génie des Procédés (PROGEP): Toulouse, 1996; Vol. 1, pp 135−140.

(8) Dixit, A. B.; Colônia, E. J.; Tavare, N. S. Use of a hydrotrope in selective precipitation of *o*- and *p*-chlorobenzoic acids. *Proceedings of the IChemE Jubilee Research Event*, Nottingham; Institution of Chemical Engineers: Rugby, U.K., 1997; Vol. 2, pp 1141−1144.

(9) Lashanizadegan, A.; Tavare, N. S. Dissociation extractive crystallization: Separation of *o*- and *p*-chlorobenzoic acids. *Proceedings of the IChemE Research Event*, Leeds; Institution of Chemical Engineers: Rugby, U.K., 1996; Vol. 1, pp 298−301.

(10) Lashanizadegan, A.; Newsham D. M. T.; Tavare, N. S. Separation of chlorobenzoic acids by dissociation extractive crystallization. *Chem. Eng. Sci.*, in press.

(11) Geetha, K. K.; Tavare, N. S.; Gaikar, V. G. Separation of *o*- and *p*-chloronitrobenzenes through hydrotropy. *Chem. Eng. Commun.* **1991**, *102*, 211−224.